Electron-impact double ionization of He by applying the Jacobi matrix approach to the Faddeev-Merkuriev equations

M. Silenou Mengoue,[1,2,*] M. G. Kwato Njock,[1] B. Piraux,[2] Yu. V. Popov,[3] and S. A. Zaytsev[4]

[1]*Centre for Atomic, Molecular Physics and Quantum Optics, Faculty of Science,*
University of Douala, P.O. Box 8580, Douala, Cameroon
[2]*Institute of Condensed Matter and Nanosciences, Université catholique de Louvain,*
Bâtiment de Hemptinne, 2, chemin du cyclotron, B1348 Louvain-la Neuve, Belgium
[3]*Nuclear Physics Institute, Moscow State University, Moscow, RU-119991, Russia*
[4]*Pacific National University, Khabarovsk, RU-680035, Russia*

We apply the Jacobi matrix method to the Faddeev-Merkuriev differential equations in order to calculate the three-body wave function that describes the double continuum of an atomic two-electron system. This function is used to evaluate within the first-order Born approximation, the fully differential cross sections for $(e,3e)$ processes in helium. The calculations are performed in the case of a coplanar geometry in which the incident electron is fast and both ejected electrons are slow. Quite unexpectedly, the results obtained by reducing our double-continuum wave function to its asymptotic expression are in satisfactory agreement with all the experimental data of Lahham-Bennani *et al.* [A. Lahaman-Bennani *et al.*, Phys. Rev. A **59**, 3548 (1999); A. Kheifets *et al.*, J. Phys. B **32**, 5047 (1999).] without any need for renormalizing the data. When the full double-continuum wave function is used, the agreement of the results with the experimental data improves significantly. However, a detailed analysis of the calculations shows that full convergence in terms of the basis size is not reached. This point is discussed in detail.

I. INTRODUCTION

The three-body Coulomb problem is one of the fundamental problems of theoretical physics which, to date, remain unsolved. A typical example of a three-body Coulomb system is helium. Despite its apparent simplicity, neither its classical nor its quantum dynamics are integrable. This loss of integrability, which is due to the electron-electron interactions, renders the two-electron dynamics in general irregular and chaotic with only small regions of regular motion in the classical phase space. Quantum mechanically, the repulsive interaction between the two electrons is responsible for the autoionization of the doubly excited states and leads to a highly structured energy spectrum with a spectral density that increases dramatically very close to the double-ionization threshold. This region of the energy spectrum just below the double-ionization threshold is presently the focus of many studies (see, for example, [1,2]).

In the present contribution, we are interested in exploring the spectral region just above the double-ionization threshold. One way of proceeding is to study $(\gamma,2e)$ processes in helium. Indeed, the double ionization leads, in this case, to a final state which is a pure two-electron continuum. Kinematically completely determined experiments have been performed by Bräuning *et al.* [3]. Except for asymmetric electron energy sharing, the corresponding absolute data are in good agreement with the results of various theoretical treatments. The time-independent ones include the convergent close-coupling (CCC) approach [4,5], the hyperspherical R-matrix approach [6,7] with semiclassical outgoing wave

(HRM-SOW), the exterior complex scaling (ECR) method [8], and the flux formula [9]. More recently, time-dependent approaches have also been developed. They include the wave-packet-evolution approach [10], the time-dependent close-coupling method [11], and the Jacobi matrix calculations of Foumouo *et al.* [12]. All these methods differ by how the electronic correlations which result from the electron-electron interaction are described. However, the good agreement of the experimental data with all the theoretical results obtained with these methods seems to suggest that the electronic correlations in the final state do not play a crucial role in this context.

The situation described above contrasts with the $(e,3e)$ processes. For very high energies of the incident electron and very small momentum transfers, that is to say, in the dipole limit, the target final state is again a double continuum. As for $(\gamma,2e)$ processes, kinematically completely determined experiments have been performed. Fully resolved fivefold differential cross sections (5DCSs) of double ionization of helium by 5.6 keV electron impact have been measured by Lahmam-Bennani *et al.* [4,13]. They considered asymmetric coplanar geometries and symmetric energy sharing between the two ejected electrons at an excess energy of 8 and 20 eV with 0.22 and 0.24 a.u. momentum transfer, respectively. Upon these kinematical conditions and in particular for the lowest value of the excess energy, all theoretical results [4,10,14–16] show significant discrepancies, mainly concerning the magnitude of the cross section. In addition, most of these results do not agree well with the absolute experimental data. Possible reasons to explain those discrepancies are the following. First, it is possible that the first-order Born approximation, which, in the dipole limit, is expected to work, is not sufficient and that higher-order terms become significant. This may be the case when both electrons are ejected in the backward direction

*smengoue@yahoo.fr

where the residual ion carries a large momentum. Second, the use of initial- and final-state wave functions that do not satisfy the Kato cusp conditions may introduce spurious effects in the transition amplitude. Third, the correct asymptotic behavior of the multichannel final-state wave function is not known, requiring necessarily some approximations. The validity of the first-order Born approximation has been studied by Kheifets and Bray. They showed [5] that, in the conditions of the experiments of Lahmam-Bennani, the contribution of the second Born term is actually negligible, at least in the vicinity of the main peaks. The role of the cusp conditions in $(e,3e)$ processes has been investigated by Chuluunbaatar *et al.* [17]. They concluded that in the experiments of Lahmam-Bennani *et al.*, the cusp conditions do not play any appreciable role. Finally, Serov *et al.* [10] have shown that it is not essential to use a final double-continuum wave function which has the correct asymptotic behavior. They compared the CCC results obtained with a double-continuum wave function that has an incorrect asymptotic behavior with the results of their time-dependent approach in which the final wave packet evolves until it reaches the asymptotic region. Having found similar results, they concluded that the disagreement between the CCC results and the experimental data is not due to the incorrect asymptotic behavior of the CCC double-continuum wave function. This discussion seems to suggest that the way electron-electron correlations are described in the final electron double-continuum wave function at moderate distances is actually at the origin of the discrepancies between theory and experiments.

In this paper, we use the Jacobi matrix approach to the Faddeev-Merkuriev differential equations to generate a correlated three-charged particle continuum wave function in which the two-body subdomains are treated correctly. We apply this method to the calculation, within the first-order Born approximation, of the 5DCS for electron-impact double ionization of helium in the small momentum transfer regime. A similar method based on Faddeev-Merkuriev integral equations has been successfully used by Papp *et al.* in many different contexts as, for instance, the description of bound [18] and resonance states [19–21] of three-body Coulomb systems or electron-hydrogen scattering [22]. Note that in the cases treated by Papp *et al.*, the kernel of the Faddeev-Merkuriev integral equation is compact, giving a convergence of the results as a function of the size of the basis. Recently, Zaytsev *et al.* used the present approach to treat $(e,2e)$ and $(e,3e)$ processes in helium [16,23]. In the case of the $(e,2e)$ processes, they considered single ionization with and without excitation of the residual ion and demonstrated the convergence of the results as a function of the basis size [23]. In the case of the $(e,3e)$ processes, such a convergence analysis has not been shown. However, this analysis is pertinent, since the present approach involves a Lippmann-Schwinger equation with a noncompact kernel. In this paper, this point is discussed in detail.

This paper is organized as follows. After this Introduction, we briefly review the theoretical approach used to generate the double-continuum wave function in Sec. II. In Sec. III A, we give some technical details about how we calculate the 5DCS for the $(e,3e)$ process we study in helium. Section III B is devoted to the results. We first calculate these cross sections by reducing the double-continuum wave function to its asymptotic expression and compare the results with all the experimental data of Lahmam-Bennani *et al.* [4,13] at 5.6 keV electron incident energy. Then, we use the full double-continuum wave function to evaluate these 5DCSs and compare the results to both the experimental data and the results obtained with other theoretical approaches. Finally, in Sec. III C, we study the convergence of our results as a function of the basis parameters. Unless explicitly stated, we use atomic units throughout this paper.

II. DOUBLE CONTINUUM WAVE FUNCTION: THEORY

The two-electron continuum wave function with an asymptotic ingoing wave behavior is a solution of the following Schrödinger equation:

$$\left[E + \frac{1}{2}\Delta_1 + \frac{1}{2}\Delta_2 + \frac{Z}{r_1} + \frac{Z}{r_2} - \frac{1}{r_{12}} \right]$$
$$\times \Psi^{(-)}(\mathbf{k}_1,\mathbf{k}_2; \mathbf{r}_1,\mathbf{r}_2) = 0, \quad (1)$$

where $\mathbf{r}_1$ and $\mathbf{r}_2$ are the position vectors of electrons 1 and 2, and $\mathbf{k}_1$ and $\mathbf{k}_2$ their corresponding momentum. $r_{12} = |\mathbf{r}_2 - \mathbf{r}_1|$ is the interelectronic distance. $Z = 2$ denotes the charge of the infinitely massive nucleus, the position of which coincides with the origin of the laboratory system. E is the total energy of the two electrons. Following Merkuriev and Faddeev [24], we split the electron-nucleus Coulomb potentials into a short- and a long-range part:

$$\frac{Z}{r_i} = V_i^{(s)}(r_1,r_2) + V_i^{(l)}(r_1,r_2), \quad (2)$$

where

$$V_i^{(s)}(r_1,r_2) = \frac{Z}{r_i}\zeta(r_i,r_j), \quad V_i^{(l)}(r_1,r_2) = \frac{Z}{r_i}[1 - \zeta(r_i,r_j)],$$
$$(3)$$

and

$$\zeta(r_i,r_j) = 2/\{1 + \exp[(r_i/a)^\nu/(1 + r_j/b)]\}. \quad (4)$$

The subscripts i and j take the value 1 or 2 with $i \neq j$. The role of $\zeta(r_i,r_j)$ is to fix a border between Ω_0, the so-called true three-body scattering region (where $r_1 \sim r_2$), and the two-body scattering regions Ω_1 $(r_1 \gg r_2)$ or Ω_2 $(r_2 \gg r_1)$. Note that although the function $\zeta(r_i,r_j)$ depends on the three adjustable parameters a, b, and ν, the final results should not depend on the choice of these parameters.

The fact that the two electrons are identical particles allows us to introduce the new functions $\Psi_i^{(-)}(\mathbf{k}_1,\mathbf{k}_2; \mathbf{r}_1,\mathbf{r}_2)$ $(i = 1,2)$, such that $\Psi^{(-)} = (1/\sqrt{2})[\Psi_1^{(-)} + \Psi_2^{(-)}]$. Taking into account the exchange symmetry of the solution of Eq. (1), $\Psi^{(-)}(\mathbf{k}_1,\mathbf{k}_2; \mathbf{r}_1,\mathbf{r}_2) = g\Psi^{(-)}(\mathbf{k}_1,\mathbf{k}_2; \mathbf{r}_2,\mathbf{r}_1)$, where $g = +1 (-1)$ for a singlet (triplet) state, we have

$$\Psi_2^{(-)}(\mathbf{k}_1,\mathbf{k}_2; \mathbf{r}_1,\mathbf{r}_2) = g\widehat{P}_{12}\Psi_1^{(-)}(\mathbf{k}_1,\mathbf{k}_2; \mathbf{r}_1,\mathbf{r}_2). \quad (5)$$

We now demand that the functions $\Psi_1^{(-)}$ and $\Psi_2^{(-)}$ satisfy the following equations of Faddeev type:

$$\left[E + \frac{1}{2}\Delta_1 + \frac{1}{2}\Delta_2 + V_1^{(l)} + V_2^{(l)} - \frac{1}{r_{12}} \right] \Psi_1^{(-)}$$
$$= -\sqrt{2}\, V_2^{(s)} \Psi^{(-)}, \qquad (6)$$

$$\left[E + \frac{1}{2}\Delta_1 + \frac{1}{2}\Delta_2 + V_1^{(l)} + V_2^{(l)} - \frac{1}{r_{12}} \right] \Psi_2^{(-)}$$
$$= -\sqrt{2}\, V_1^{(s)} \Psi^{(-)}. \qquad (7)$$

According to the previous discussion, we can rewrite Eq. (6) as

$$\left[E + \frac{1}{2}\Delta_1 + \frac{1}{2}\Delta_2 + V_1^{(l)} + V_2^{(l)} - \frac{1}{r_{12}} \right] \Psi_1^{(-)}$$
$$= -V_2^{(s)}(1 + g\widehat{P}_{12})\Psi_1^{(-)}, \qquad (8)$$

since $\Psi^{(-)} = 1/\sqrt{2}[1 + g\widehat{P}_{12}]\Psi_1^{(-)}$. Equation (7) can be transformed in exactly the same way. As a result, we obtain only one equation for the component $\Psi_1^{(-)}(\mathbf{k}_1, \mathbf{k}_2; \mathbf{r}_1, \mathbf{r}_2)$, which is fully equivalent to Eq. (1). Let us now rewrite Eq. (8) in the following way:

$$\left[E + \frac{1}{2}\Delta_1 + \frac{1}{2}\Delta_2 + \frac{Z-1}{r_1} + \frac{Z}{r_2} \right] \Psi_1^{(-)} = V(\mathbf{r}_1, \mathbf{r}_2)\Psi_1^{(-)}, \qquad (9)$$

where

$$V(\mathbf{r}_1, \mathbf{r}_2) = \frac{1}{r_{12}} - V_1^{(l)}(r_1, r_2) + \frac{Z-1}{r_1} - gV_2^{(s)}(r_1, r_2)\widehat{P}_{12}. \qquad (10)$$

It is straightforward to see that the potential $V(\mathbf{r}_1, \mathbf{r}_2)$ is short range in the two-body scattering region Ω_1 ($r_1 \gg r_2$).

Equation (9) is the basic equation for the numerical calculation of the double-continuum wave function. Instead of solving this equation directly, however, it is more convenient to transform it into the following integral equation of Lippmann-Schwinger type:

$$\Psi_1^{(-)}(\mathbf{k}_1, \mathbf{k}_2; \mathbf{r}_1, \mathbf{r}_2)$$
$$= [\varphi^{(-)}(\mathbf{k}_2, \mathbf{r}_2; Z) \varphi^{(-)}(\mathbf{k}_1, \mathbf{r}_1; Z-1)\theta(k_1 - k_2)$$
$$+ g\varphi^{(-)}(\mathbf{k}_1, \mathbf{r}_2; Z) \varphi^{(-)}(\mathbf{k}_2, \mathbf{r}_1; Z-1)\theta(k_2 - k_1)]$$
$$+ \int\int d\mathbf{r}_1' \, d\mathbf{r}_2' \, G^{(-)}(\mathbf{r}_1, \mathbf{r}_2; \mathbf{r}_1', \mathbf{r}_2'; E)$$
$$\times V(\mathbf{r}_1', \mathbf{r}_2') \Psi_1^{(-)}(\mathbf{k}_1, \mathbf{k}_2; \mathbf{r}_1', \mathbf{r}_2'). \qquad (11)$$

This new equation incorporates the boundary conditions through the Green's function $G^{(-)}$ associated with the operator of the left-hand side of Eq. (9). This operator describes two independent subsystems, namely, an electron in the field of a nucleus of charge Z and another electron in the field of a nucleus of charge $Z - 1$. The first term in the square brackets in the right-hand side of Eq. (11) is the solution of Eq. (9) without the right-hand-side term (the homogeneous equation). In principle, this term describes the two electrons asymptotically, since the potential $V(\mathbf{r}_1, \mathbf{r}_2)$ is short range. However, this is only true in the two-body scattering region Ω_1 and not necessarily in the three-body scattering region Ω_0. This and the fact that both electrons are not symmetrically

described led us to the introduction of an ansatz for this term, the choice of which was inspired by the method of the effective charges [25] in the same spirit as in the Jacobi matrix approach [26]. This ansatz involves a product of two Coulomb waves $\varphi^{(-)}(\mathbf{k}_i, \mathbf{r}_2; Z)\, \varphi^{(-)}(\mathbf{k}_j, \mathbf{r}_1; Z-1)$ describing a slow escaping electron which, being closer to the ion, "sees" its full charge Z and a fast electron which, being far from both the nucleus and the slow electron, sees a charge $Z - 1$. The step functions θ with $\theta(0) = 1/2$ are introduced to ensure that when $k_1 > k_2$, the fast electron momentum k_1 is associated with the effective charge $Z - 1$ and k_2 to Z and vice versa if $k_1 < k_2$. When $k_1 = k_2$, k_1 can be associated with either Z or $Z - 1$.

Green's function $G^{(-)}$ can be evaluated as a convolution integral along a contour $\mathcal{C}$ in the complex energy $\mathcal{E}$ plane:

$$G^{(-)}(\mathbf{r}_1, \mathbf{r}_2; \mathbf{r}_1', \mathbf{r}_2'; E)$$
$$= \frac{1}{2\pi i} \int_{\mathcal{C}} d\mathcal{E}\, g^{(-)}(\mathbf{r}_1, \mathbf{r}_1'; \mathcal{E} - i0; Z-1)$$
$$\times g^{(-)}(\mathbf{r}_2, \mathbf{r}_2'; E - \mathcal{E} - i0; Z). \qquad (12)$$

For the time being, the contour $\mathcal{C}$ runs from $-\infty$ to $+\infty$ along the real axis of the complex $\mathcal{E}$ plane. We now perform a partial wave decomposition of the wave function $\Psi_1^{(-)}$ and write

$$\Psi_1^{(-)}(\mathbf{k}_1, \mathbf{k}_2; \mathbf{r}_1, \mathbf{r}_2) = \frac{2}{\pi} \frac{1}{k_1 k_2} \sum_{L,M,\lambda_0,l_0} \left\{ \psi_{l_0\lambda_0}^{LM}(\mathbf{r}_1, \mathbf{r}_2; k_1, k_2) \right.$$
$$\times \mathcal{Y}_{l_0\lambda_0}^{LM*}(\widehat{\mathbf{k}}_1, \widehat{\mathbf{k}}_2)\, \theta(k_1 - k_2)$$
$$+ g\, \psi_{l_0\lambda_0}^{LM}(\mathbf{r}_1, \mathbf{r}_2; k_2, k_1)$$
$$\left. \times \mathcal{Y}_{l_0\lambda_0}^{LM*}(\widehat{\mathbf{k}}_2, \widehat{\mathbf{k}}_1)\, \theta(k_2 - k_1) \right\}. \qquad (13)$$

L is the total angular momentum and M its projection on the quantization axis. l_0 and λ_0 are the individual angular momenta of the two electrons. $\mathcal{Y}_{l_0\lambda_0}^{LM}(\widehat{\mathbf{p}}, \widehat{\mathbf{q}})$ is the bipolar harmonics. The partial wave function $\psi_{l_0\lambda_0}^{LM}$ in Eq. (13) can be further expanded in a basis of Coulomb Sturmian functions [12] and bipolar harmonics:

$$\psi_{l_0\lambda_0}^{LM}(\mathbf{r}_1, \mathbf{r}_2) = \sum_{l,\lambda,n,\nu} C_{n\nu}^{L(l\lambda)}(E)\, \langle \mathbf{r}_1, \mathbf{r}_2 | n\, l\, \nu\, \lambda;\, LM \rangle, \qquad (14)$$

with

$$\langle \mathbf{r}_1, \mathbf{r}_2 | n\, l\, \nu\, \lambda;\, LM \rangle = \frac{\phi_{nl}^{\kappa}(r_1)}{r_1} \frac{\phi_{\nu\lambda}^{\kappa}(r_2)}{r_2} \mathcal{Y}_{l\lambda}^{LM}(\widehat{\mathbf{r}}_1, \widehat{\mathbf{r}}_2). \qquad (15)$$

The Coulomb Sturmian functions $\phi_{\nu\lambda}^{\kappa}(r)$ form a complete and discrete set of $\mathcal{L}^2$-integrable functions defined as follows:

$$\phi_{\nu\lambda}^{\kappa}(r) = \left[\frac{\kappa(\nu - \lambda - 1)!}{\nu(\nu + \lambda)!} \right]^{1/2} (2\kappa r)^{\lambda+1} e^{-\kappa r} L_{\nu-\lambda-1}^{2\lambda+1}(2\kappa r),$$
$$\nu \geqslant 1 + \lambda, \qquad (16)$$

where $L_n^{\alpha}(x)$ is a Laguerre polynomial. κ is a nonlinear parameter which plays the role of a dilation parameter. These functions are known to be orthogonal with the weight $1/r$, that is,

$$\int_0^{\infty} \frac{dr}{r} \phi_{\nu\lambda}^{\kappa}(r)\phi_{\nu'\lambda}^{\kappa}(r) = \frac{\kappa}{\nu}\delta_{\nu\nu'},$$

and lead to a representation of the Coulomb potential in the form of an infinite tridiagonal (Jacobi) matrix [27]. Note, that

any radial Coulomb eigenstate $\varphi_{\alpha\,l}(r; Z)$ can be expanded into a series of Sturmian functions:

$$\varphi_{\alpha l}(r; Z) = \sum_{\nu} \mathcal{S}_{\nu l}(\alpha, Z) \phi_{\nu l}^{\kappa}(r). \qquad (17)$$

For the continuum states we are concerned with, the expansion coefficient takes the following form:

$$\begin{aligned}
\mathcal{S}_{\nu l}(k; Z) = & \left[\frac{\nu(\nu + l)!}{\kappa(\nu - l - 1)!} \right]^{1/2} 2^l (\sin \zeta)^{l+1} \\
& \times e^{-\pi t/2} \xi^{-it} \frac{|\Gamma(l + 1 - it)|}{(2l + 1)!} \\
& \times (\xi)^{-(\nu - l - 1)} {}_2F_1(-\nu + l + 1, l + 1 \\
& - it; 2l + 2; 1 - \xi^2),
\end{aligned} \qquad (18)$$

where $t = -Z/k$ and $\xi = \exp(i\zeta) = (ik - \kappa)/(ik + \kappa)$. Finally, from Eq. (11), we obtain the following system of equations for the coefficients $C_{n\nu}^{L(l\lambda)}(k_1, k_2)$:

$$\begin{aligned}
C_{n\nu}^{L(l\lambda)}(k_1, k_2) = & \; i^{l_0 + \lambda_0} \delta_{(l\lambda)(l_0\lambda_0)} e^{-i[\sigma_{l_0}(k_1, Z-1) + \sigma_{\lambda_0}(k_2, Z)]} \\
& \times \mathcal{S}_{n l_0}(k_1, Z-1) \mathcal{S}_{\nu\lambda_0}(k_2, Z) \\
& + \sum_{n'\nu', n''\nu''=0}^{N-1} \left[\frac{1}{2\pi i} \int_{\mathcal{C}} d\mathcal{E} \, g_{nn'}^{(-)l}(\mathcal{E}, Z-1) \right. \\
& \times \left. g_{\nu\nu'}^{(-)\lambda}(E - \mathcal{E}, Z) \right] \sum_{l''\lambda''} V_{n'\nu', n''\nu''}^{L(l\lambda)(l''\lambda'')} C_{n''\nu''}^{L(l''\lambda'')}(E),
\end{aligned} \qquad (19)$$

where

$$V_{n\nu, n'\nu'}^{L(l\lambda)(l'\lambda')} = \langle n\, l\, \nu\, \lambda; \; LM | \, V(\mathbf{r}_1, \mathbf{r}_2) \, | n'\, l'\, \nu'\, \lambda'; \; LM \rangle$$

denotes a matrix element of the potential defined by Eq. (10) in the basis (15). The upper limit in the sum in Eq. (19) means that the matrix elements of the short-range potential are assumed to be zero for any value of the index n exceeding $(N - 1)$. The partial Coulomb Green's function $g^{(\pm)l}(r, r'; E; Z)$ can be represented by a sum over the Coulomb eigenstates $\varphi_{\alpha\,l}(r; Z)$ as follows:

$$g^{(\pm)l}(r, r'; E; Z) = \sum_{\alpha} \frac{\varphi_{\alpha l}^*(r; Z) \varphi_{\alpha l}(r'; Z)}{E - \varepsilon_{\alpha} \pm i0}, \qquad (20)$$

Keeping in mind the decomposition (17) of the Coulomb eigenfunctions, the contour integral in Eq. (19) becomes

$$\begin{aligned}
& \frac{1}{2\pi i} \int_{\mathcal{C}} d\mathcal{E} \, g_{nn'}^{(-)l}(\mathcal{E}, Z-1) \, g_{\nu\nu'}^{(-)\lambda}(E - \mathcal{E}, Z) \\
& = \sum_{\alpha} \mathcal{S}_{nl}^*(\alpha, Z-1) \mathcal{S}_{n'l}(\alpha, Z-1) \, g_{\nu\nu'}^{(-)\lambda}(E - \varepsilon_{\alpha}, Z). \quad (21)
\end{aligned}$$

At this point we could apply Eq. (20) again and obtain a double summation-integration in (21), but it is not convenient for the numerical calculations. It is useful now to remember the following representation for the matrix element $g_{\nu\nu'}^{(\pm)\lambda}(E)$ [28]:

$$g_{\nu\nu'}^{(\pm)\lambda}(E; Z) = -\frac{2}{p} \mathcal{S}_{\nu_<\lambda}(p, Z) \mathcal{C}_{\nu_>\lambda}^{(\pm)}(p, Z), \quad \nu_< = \min\{\nu, \nu'\},$$

$$\nu_> = \max\{\nu, \nu'\}, \qquad (22)$$

with $p = \sqrt{2E}$. $\mathcal{C}_{nl}^{(\pm)}(p, Z)$ is a Pollaczek function that can be written as follows [27,29]:

$$\begin{aligned}
\mathcal{C}_{nl}^{(\pm)}(p, Z) = & -\left[\frac{n(n + l)!}{\kappa(n - l - 1)!} \right]^{1/2} \frac{(n - l - 1)! \, e^{\pi t/2} \xi^{it}}{(2 \sin \zeta)^l} \\
& \times \frac{\Gamma(l + 1 \mp it)}{|\Gamma(l + 1 \mp it)|} \frac{(\xi)^{\mp(n-l)}}{\Gamma(n + 1 \mp it)} \\
& \times {}_2F_1(-l \mp it, n - l; \; n + 1 \mp it; \; \xi^{\mp 2}). \quad (23)
\end{aligned}$$

The function $\mathcal{C}_{nl}^{(+)}(p, Z) [\mathcal{C}_{nl}^{(-)}(p, Z)]$ is determined for $\text{Im}(p) > 0 \; [\text{Im}(p) < 0]$ in the complex p plane and the analytical continuation writes [29]

$$\mathcal{C}_{nl}^{(+)}(p, Z) = \mathcal{C}_{nl}^{(-)}(p, Z) + 2i \mathcal{S}_{nl}(p, Z). \qquad (24)$$

Equation (21) can be effectively used if $E < 0$, i.e., for low-energy $(e, 2e)$ reactions. Details are presented in [23]. For $(e, 3e)$ reactions, $E > 0$ and the direct evaluation of the contour integral in Eq. (19) can be performed rotating the contour of integration. This method was proposed by Shakeshaft [30] and its application to our case is explained in [23]. We only give the final result here. For this purpose, we first move from the energy to the momentum space. For the sake of clarity, we change the notations: we replace $g_{\nu\nu'}^{(\pm)\lambda}(E; Z)$ by $\mathcal{G}_{\nu\nu'}^{\lambda(-)}(p; Z)$ and rewrite the matrix element of the three-body Green's function (12) in the basis (16) as follows:

$$\begin{aligned}
G_{nn', \nu\nu'}^{l\lambda(-)}(E) = & \frac{1}{4\pi i} \int_{\mathcal{C}} d\mathcal{E} \, \mathcal{G}_{nn'}^{l(-)}(\sqrt{\mathcal{E}_0 + \mathcal{E}}; Z - 1) \\
& \times \mathcal{G}_{\nu\nu'}^{\lambda(-)}(\sqrt{\mathcal{E}_0 - \mathcal{E}}; Z). \quad (25)
\end{aligned}$$

Where $\mathcal{E}_0 = E$. Now we rotate the contour $\mathcal{C}$ by a positive angle φ. This may be done by the following change of variable $\mathcal{E} \to \mathcal{E}_0 e^{i\varphi} t$ with t real and varying from $-\infty$ to $+\infty$. This new contour crosses cuts of both Green's functions in the complex $\mathcal{E}$ plane. By using the analytical continuation (24) while integrating along unphysical sheets, we arrive at the expression

$$\begin{aligned}
G_{nn', \nu\nu'}^{l\lambda(-)}(E) = & \frac{\mathcal{E}_0 e^{i\varphi}}{4\pi i} \left\{ \int_{-\infty}^{0} dt \, \mathcal{G}_{nn'}^{l(-)}(k; Z-1) \left[\mathcal{G}_{\nu\nu'}^{\lambda(+)}(p; Z) \right. \right. \\
& + \left. \frac{4i}{p} \mathcal{S}_{\nu\lambda}(p; Z) \mathcal{S}_{\nu'\lambda}(p; Z) \right] \\
& + \int_{0}^{\infty} dt \left[\mathcal{G}_{nn'}^{l(+)}(k; Z-1) + \frac{4i}{k} \mathcal{S}_{nl}(k; Z-1) \right. \\
& \times \left. \left. \mathcal{S}_{n'l}(k; Z-1) \right] \mathcal{G}_{\nu\nu'}^{\lambda(-)}(p; Z) \right\}, \quad (26)
\end{aligned}$$

where $k = \sqrt{\mathcal{E}_0(1 + t e^{i\varphi})}$, and $p = \sqrt{\mathcal{E}_0(1 - t e^{i\varphi})}$. This last integral is calculated fully numerically and we checked that the results do not depend on the angle φ.

III. $(e, 3e)$ PROCESSES IN HELIUM

A. First-order approach

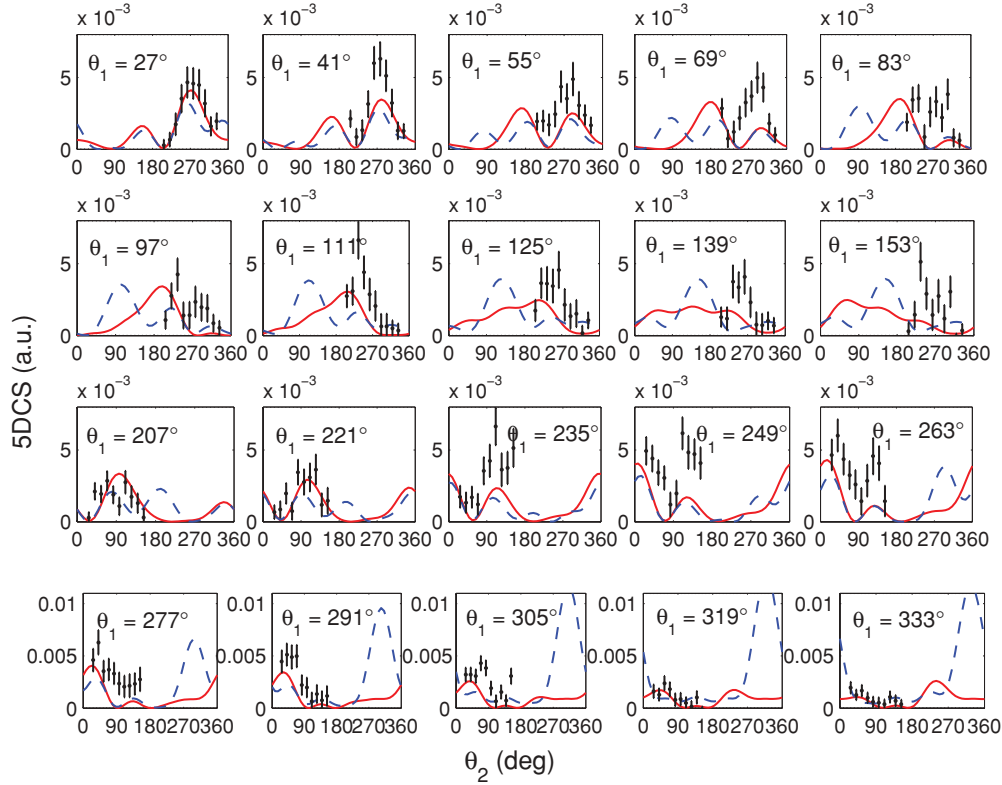The theoretical approach described above to calculate double-continuum wave functions is now applied to $(e, 3e)$

FIG. 1. (Color online) Fully fivefold differential cross section (5DCS) for electron-impact double-ionization reaction $He(e,3e)He^{++}$. The incident energy is $E_0 = 5599$ eV and the energies of the slow ejected electrons are $E_1 = E_2 = 10$ eV. The scattering angle θ_s of the fast incident electron is fixed and equal to $0.45°$ while the angles of the ejected electrons are θ_1 and θ_2. One of these angles, θ_1, is fixed and the other varies. The blue dashed line is our result obtained by means of a zero-order calculation. The red solid line is the result obtained by solving the Lippmann-Schwinger equation (11) for the double-continuum wave function. The solid dots with error bars are the absolute experimental data of Lahmam-Bennani [4].

processes in helium. Here, we consider the case of very high incident energies and small momentum transfer. In this dipole limit, it is expected that a first-order Born treatment is sufficient. The 5DCS which is the most differential one is given by

$$\sigma^{(5)} \equiv \frac{d^5\sigma}{d\Omega_s\, dE_1\, d\Omega_1\, dE_2\, d\Omega_2}$$

$$= \frac{4p_s p_1 p_2}{p_i} \frac{1}{K^4} \mid \langle \Psi^{(-)}(\mathbf{p}_1,\mathbf{p}_2)| \exp(i\mathbf{K}\cdot\mathbf{r}_1)$$

$$+ \exp(i\mathbf{K}\cdot\mathbf{r}_2) - 2|\Psi_0\rangle \mid^2 , \qquad (27)$$

where $(E_i,\mathbf{p_i})$, $(E_s,\mathbf{p_s})$, $(E_1,\mathbf{p_1})$, and $(E_2,\mathbf{p_2})$ are the energy and momentum of the incident, scattered, and the two ejected electrons, respectively; $\mathbf{K} = \mathbf{p_i} - \mathbf{p_s}$ is the momentum transfer. Ψ_0 and $\Psi^{(-)}$ are the initial and the final double-continuum wave functions of helium. The ground-state wave function Ψ_0 is expanded in a basis of the Coulomb Sturmian functions (16) for the radial coordinates and bipolar harmonics for the angular coordinates [12]:

$$\Psi_0(\vec{r}_1,\vec{r}_2) = \sum_{l_1 l_2} \sum_{n_1 n_2} \gamma^{l_1 l_2}_{n_1 n_2} \Phi^{l_1 l_2 00}_{n_1 n_2} \mathcal{A}$$

$$\times \left(\frac{\phi^{\kappa}_{n_2 l_2}(r_2)}{r_2} \mathcal{Y}^{00}_{l_1 l_2}(\hat{r}_1,\hat{r}_2) \frac{\phi^{\kappa}_{n_1 l_1}(r_1)}{r_1} \right), \quad (28)$$

where $\Phi^{l_1 l_2 LM}_{n_1 n_2}$ is the expansion coefficient. They are obtained by diagonalizing the atomic Hamiltonian in Eq. (1). $\mathcal{A}$ projects onto either singlet or triplet states in order to ensure the symmetry or antisymmetry of the spatial wave function as required by the Pauli principle. The coefficient $\gamma^{l_1 l_2}_{n_1 n_2} = 1 + (1/\sqrt{2} - 1)\delta^{l_1 l_2}_{n_1 n_2}$ controls the redundancies which, from the exchange of the electrons, may occur in the basis. In the present calculation, n_1, n_2 vary from 1 to 15 and l_1, l_2 from 0 to 3. By choosing the nonlinear parameter $\kappa_0 = 2$, we obtain $E_0 = -2.90327$ a.u. for the ground-state energy [31].

B. Results and discussion

In this section, we present results on the 5DCS [Eq. (27)]. We consider the same kinematics as in the experiments of Lahmam-Bennani *et al.* [4,13] where the geometry of the $(e,3e)$ process is coplanar asymmetric and both ejected electrons have the same energy. Two different kinematics, referred to as kinematics A and B, are considered: in kinematics A, the excess energy is equal to 20 eV and the momentum transfer to 0.24 a.u., while in kinematics B, the excess energy is 8 eV and the momentum transfer, 0.22 a.u.. The 5DCS is measured as a function of one of the ejection angles, say, θ_2 for fixed values of θ_1, the other angle.

To start our discussion, let us first calculate the 5DCS by treating the target final state at the zero order. This means

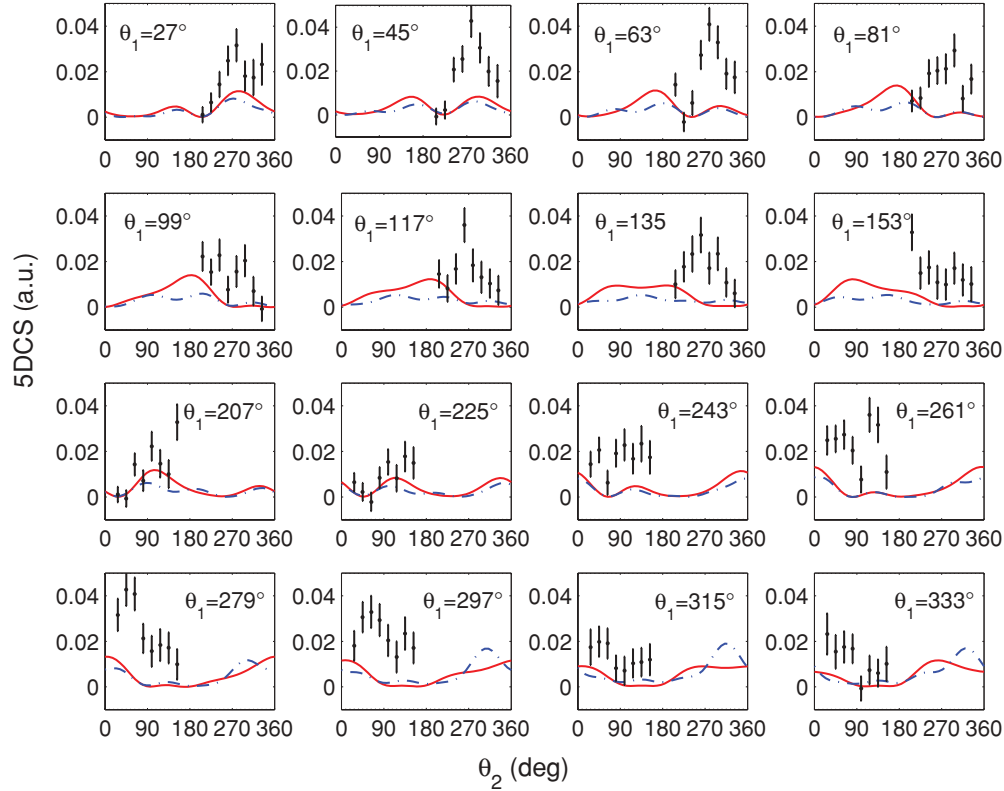FIG. 2. (Color online) Fully fivefold differential cross section (5DCS) for electron-impact double-ionization reaction $He(e,3e)He^{++}$. The incident energy is $E_0 = 5587$ eV and the energies of the slow ejected electrons are $E_1 = E_2 = 4$ eV. The scattering angle θ_s of the fast incident electron is fixed and equal to $0.45°$, while the angles of the ejected electrons are θ_1 and θ_2. One of these angles, θ_1, is fixed and the other varies. The blue dotted-dashed line is our result obtained by means of a zero-order calculation. The red solid line is the result obtained by solving the Lippmann-Schwinger equation (11) for the double-continuum wave function. The solid dots with error bars are the absolute experimental data of Lahmam-Bennani [4].

that in the Lippmann-Schwinger equation (11), we only keep the first two terms of the right-hand side and neglect the correction which involves Green's function. In other words, we describe this final state by its asymptotic expression. In these calculations, it is sufficient to take into account three values (0, 1, and 2) of the total angular momentum L and a maximum value l_{max} of 5 for the individual angular momenta. The results (the dashed line) for kinematics A and B are shown in Figs. 1 and 2, respectively. First, we see that the agreement between our results and the experimental data is better in kinematics A than in kinematics B. This is expected since in the latter case, both electrons are slower. However, it is surprising to see that the order of magnitude of our results in particular for the kinematics B is correct and does not necessitate any renormalization of the data as it is usually needed with other approaches. This contrasts with the case in which the final target state is a product of two Coulomb functions with effective charges equal to 2 and which leads to results in poor agreement with the experimental data as far as the shape and the magnitude are concerned. In the present conditions, on the other hand, this asymptotic term is unable to reproduce well the node in the final target state wave function at $\theta_1 = \theta_2$ (in kinematics A) when both ejected electrons share exactly the same energy and especially when they are ejected backward.

In Figs. 1 and 2, we also present our results (solid red line) obtained by solving the Lippmann-Schwinger equation (11) for the double-continuum wave function. In that case, we use three values (0, 1, and 2) of the total angular momentum L and a maximum value of 3 for the individual angular momenta. The number N of Coulomb Sturmian functions is 25 with the dilation parameter $\kappa = 0.6$ for kinematics A and 30 with $\kappa = 0.4$ for kinematics B. The parameters of the splitting function (4) are $a = 3$, $b = 20$, and $\nu = 2.1$. We clearly see that for both kinematics, the agreement between the experimental data and these new results has significantly improved. In particular, we see that in many cases, the node of the double-continuum wave function at $\theta_1 = \theta_2$ is better reproduced.

Let us now compare our results with those obtained with other approaches. For kinematics A, this comparison is presented in Fig. 3 for four different values of θ_1: $27°$, $97°$, $221°$, and $319°$. Our results are represented by the red solid lines. They are close to the other results in shape but not really in magnitude. Knyr *et al.* [32] used a very similar method to ours except for the number of Sturmian functions which, in their case, is limited to 20, and a different description of the ground state. Their results, given by the blue dashed line, are in general of the same order of magnitude as ours. However, we observe significant shifts of the main peaks, in particular for the highest values of θ_1. This may be due to a numerical instability
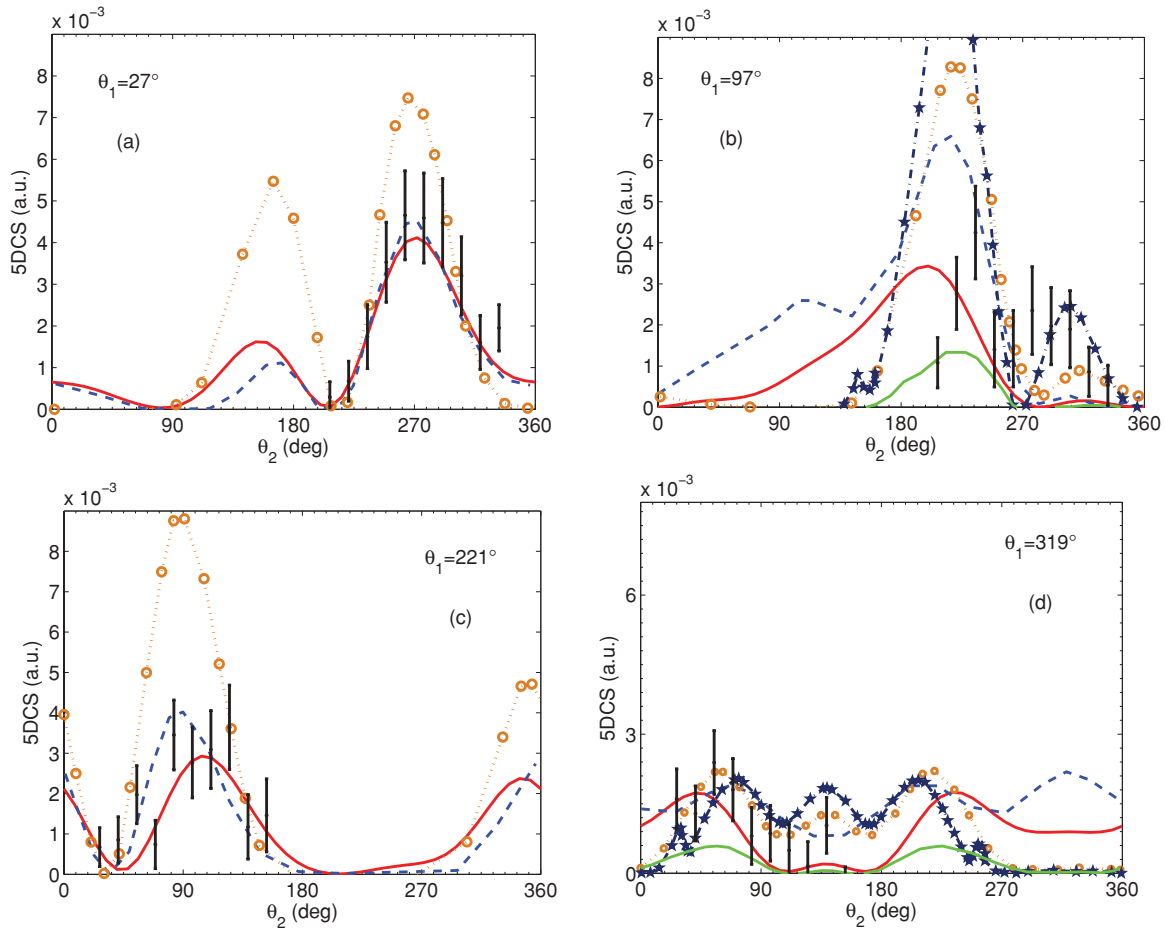
FIG. 3. (Color online) Fully five-fold differential cross section (5DCS) for electron-impact double-ionization reaction He(e,3e)He^{++}. The incident energy is $E_0 = 5599$ eV and the energies of the slow ejected electrons are $E_1 = E_2 = 10$ eV. The scattering angle θ_s of the fast incident electron is fixed and equal to $0.45°$. The 5DCS is given as a function of θ_2, the angle of one of the ejected electrons. Four values of θ_1, the angle of the other ejected electrons, are considered: $27°$ (a), $97°$ (b), $221°$ (c) and $319°$ (d). Our results given by the red solid line are compared with those obtained by other approaches: the brown dotted line with open circles are the FBA(3C) results of Jones *et al.* [15]; the blue dashed line are the results of Knyr *et al.* [32] by means of a similar method to ours; the green solid line are the CCC results (scaled up by a factor 3) of Kheifets *et al.* [4]; and the dark blue dashed line with stars are the results of Berakdar [14] by using a first-order four-body Green's function expansion. The solid dots with error bars are the absolute experimental data of Lahmam-Bennani [4].

in their calculation of the dielectronic interaction potential matrix elements. The CCC results of Kheifets *et al.* [4] are the green solid lines. In their calculations, the ground-state wave function is either a 20-term Hylleraas or a 18-term multiconfiguration Hartree-Fock wave function. Except for a small shift of the main peaks, they agree in shape with our results. However, since they are scaled up by a factor of 3, the orders of magnitude are significantly lower.

The last two curves shown in Fig. 3 were obtained by Jones *et al.* [15] (brown dotted lines with open circles) and by Berakdar [14] (dark blue dashed lines with stars). Jones *et al.* used the FBA(3C) model, namely, the first-order Born approximation with the Brauner, Briggs, and Klar (BBK) wave function [33] to describe the two ejected electrons and the Pluvinage function for the ground-state wave function. It is worth mentioning that the BBK wave function describes correctly both ejected electrons only in the asymptotic zone. Berakdar used a first-order four-body Green's function expansion formalism. The Jones and Berakdar calculations give

results that are in qualitative agreement with all the others as far as the shape is concerned. However, the Jones results are often much higher in magnitude. The quantitative agreement of the Berakdar results with the experimental data is much better, except for $\theta_1 = 97°$.

Lahmam-Bennani *et al.* [13] performed a first-order Born calculation with a Coulomb four-body final state which describes well the long-range Coulomb interaction between the three electrons and the residual ion only in the asymptotic region far from the nucleus. However, it gives results (not shown here) that must be scaled down by a factor of 10 to be compared with the experimental data. Finally, let us mention the wave-packet evolution approach [10] of Serov. His results (not shown here) are very close in shape and magnitude to the CCC results.

Let us now move to the kinematics B. The comparison between our results and those obtained with the other approaches is shown in Fig. 4. Our calculations are the only ones that give results (the red solid lines) with the correct order of magnitude.
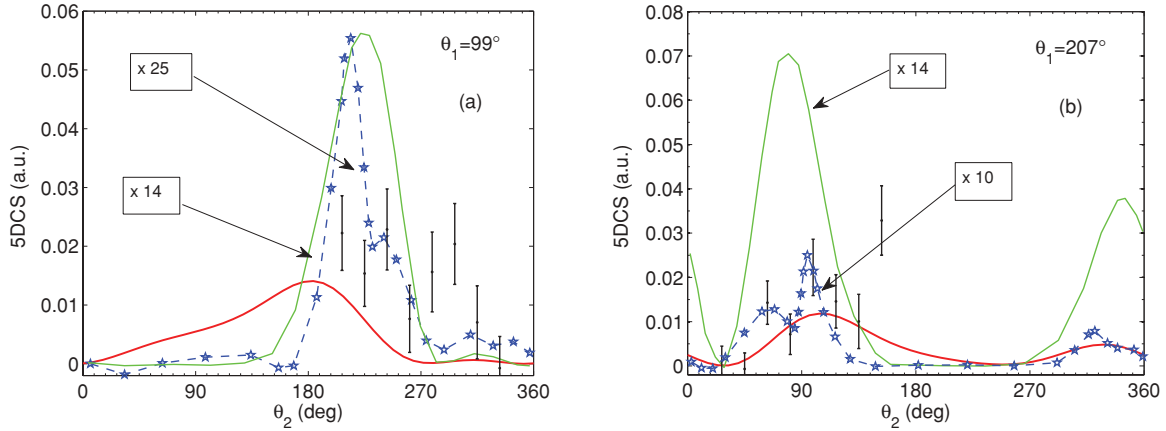
FIG. 4. (Color online) Fully fivefold differential cross section (5DCS) for electron-impact double-ionization reaction He($e,3e$)He^{++}. The incident energy is $E_0 = 5587$ eV and the energies of the slow ejected electrons are $E_1 = E_2 = 4$ eV. The scattering angle θ_s of the fast incident electron is fixed and equal to 0.45°. The 5DCS is given as a function of θ_2, the angle of one of the ejected electrons. Two values of θ_1, the angle of the other ejected electrons, are considered: 99° (a) and 207° (b). Our results (red solid line) are compared with those obtained by other approaches: the green solid line are the CCC results (scaled up by a factor 14) of Kheifets *et al.* [4] and the blue dashed line with stars are the results [scaled up by a factor 25 in (a) and 10 in (b)] of Berakdar [14] by using a first-order four-body Green's function expansion. The solid dots with error bars are the absolute experimental data of Lahmam-Bennani [4].

Let us stress that in contrast to Ref. [14], the experimental data shown in Fig. 4 are absolute and not renormalized. The results of Berakdar (blue dashed lines with stars) are in rather good qualitative agreement with the experimental data but strongly differ from these data as far as the magnitude is concerned. In the case of the CCC results (green solid line), the qualitative agreement with the experimental data is less good, while the results are also systematically much higher in magnitude. Finally, it has been reported in [34] that a first-order Born calculation using the BBK wave function for the final double continuum gives results which have to be multiplied by a large factor (around 40) to be compared with the experimental data.

C. Study of convergence

In this section, we study the convergence of our results as a function of the Coulomb Sturmian basis size. Before starting our discussion, it is worth mentioning that we have tested the calculations of the matrix elements associated with the potential (10) by using different techniques of quadrature (which are known to be very stable and fast) and checked that the results are stable even for very large values of the Sturmian function indices. The same conclusions apply to the calculation of Green's function (26). However, great care must be taken in the calculation by recursion of the Pollaczek function (23) as described in [29]. No significant change has been observed by changing the parameters of the cutoff function (4). The matrix elements associated with the dielectronic interaction potential have been evaluated by means of the method outlined in [12]. In our calculations, we chose the value of the Sturmian dilation parameter κ very close to the ejected electron velocity (in a.u.). Indeed, the dilation parameter is roughly the electron wave vector. We have checked that choosing a very small value of κ, as is usually the case in order to have spatially more extended Sturmian functions, does not help since many Sturmian functions are therefore needed to reproduce the spatial oscillations of the wave function.

The convergence of our results has been studied as a function of the number of pairs (l, λ) of electron angular momenta, as a function of the number of pairs (n, ν) of Sturmian indices for a fixed value of N (the maximum value of n or ν), and as a function of N. In Fig. 5(a), the 5DCS is shown for two values of $l_{\max}$, the maximum value of the individual electron angular momentum. Since three values of the total angular momentum L (0, 1, and 2) are taken into account, $l_{\max} = 3$ corresponds to a total number of pairs (l, λ) of 17, and 29 for $l_{\max} = 5$. The total number N of Coulomb Sturmians per electrons and per pairs (l, λ) is fixed to 25. We clearly see that the results are stable in terms of $l_{\max}$. In addition, this conclusion stays valid for higher values of N. For a fixed value of N, we checked that the results for the 5DCS converge with respect to the number of pairs (ν, n). The partial sums of each pair contribution converge to four digits of accuracy. We also used the ϵ algorithm [36] based on Padé approximants to accelerate the convergence of the partial sums. In that case, we reach at least eight digits of accuracy. In Fig. 5(b), we show the 5DCS for $l_{\max} = 3$ and three different values of N. For small values of N, it seems that the results converge. However, for larger values of N, this convergence deteriorates. It is worth mentioning that the use of the Lanczos smoothing factor σ_i^N defined in [37] does not seem to solve this problem. This suggests that the reason for the deterioration of the convergence is more fundamental.

In fact, it is directly related to the noncompactness of the kernel $(G_0 V)$ of the Lippmann-Schwinger (LS) equations [38–40] involving three or more charged particles. In the present case, the kernel of the LS equation (11) is not compact. In this respect, the fact that the potential (10) is only of finite range in the two-body scattering regions Ω_1 and Ω_2 and not in the three-body scattering region Ω_0 plays an important role. By contrast, if we use the present method to calculate the single-continuum wave functions of helium, the integral part of the LS equation is convergent due to convergent features of the single-continuum wave function, and we have
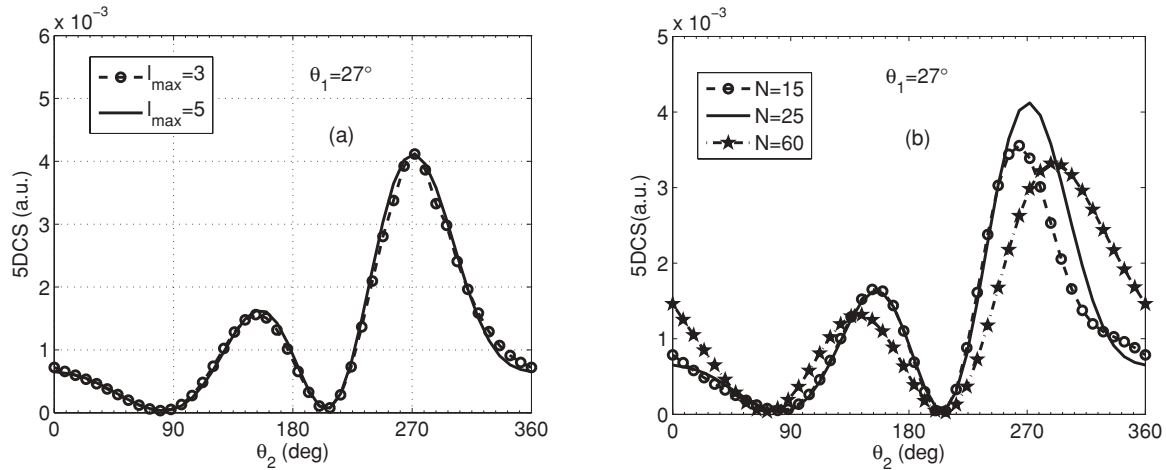
FIG. 5. Fully fivefold differential cross section (5DCS) for electron-impact double-ionization reaction He($e,3e$)He^{++}. The incident energy is $E_0 = 5599$ eV and the energies of the slow ejected electrons are $E_1 = E_2 = 10$ eV. The scattering angle θ_s of the fast incident electron is fixed and equal to $0.45°$ while the angles of the ejected electrons are θ_1 and θ_2. $\theta_1 = 27°$ and θ_2 varies. In (a), the calculations are performed for two different maximum values l_{max} of the individual electron angular momentum and for $N = 25$ where N is the total number of Coulomb Sturmian functions per electron and per individual electron angular momentum. In (b), the calculations are performed for three values of N and $l_{max} = 3$.

checked that the results for the triply differential cross section (3DCS) of single ionization (without excitation) of helium converge.

In Fig. 6, we present our results for an incident electron energy of 5500 eV, an ejected electron energy of 75 eV, and a scattering angle of $1°$. The calculations were performed for four different values of N. We clearly see that convergence is reached already for relatively small values of N. In the case of ionization excitation, Zaystev *et al.* [23] also obtained
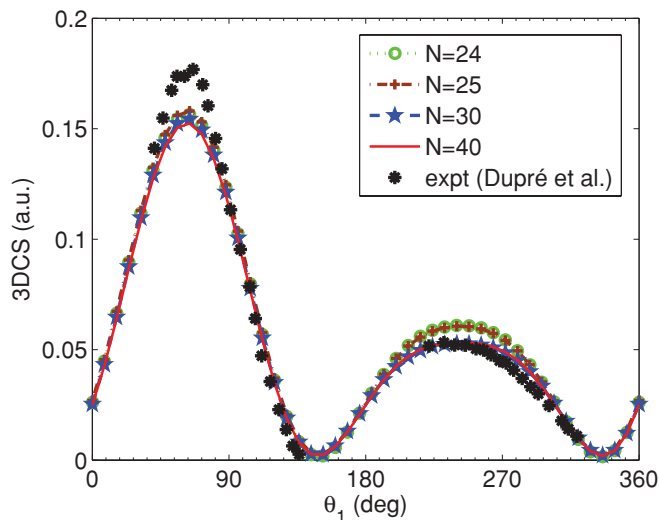

FIG. 6. (Color online) Triply differential cross section (3DCS) for electron-impact ionization of He as a function of θ_1 the electron ejection angle. The incident energy is $E_0 = 5500$ eV, the energy of the ejected electron is equal to 75 eV and the scattering angle to $1°$. The results are presented for different values of N that defines the size of the basis. The solid dots are the absolute experimental data of Dupré *et al.* [35].

convergence with a small value of N, but they had to use the Lanczos smoothing factor mentioned above.

The problem of the compactness of the kernel of the LS equations involving three or more charged particles is still the subject of current investigations by several groups [41–44]. In this context, the problem of convergence we encounter must be also present in all the approaches where the free term in the right-hand side of the LS equation (11) does not satisfy the correct three-body Coulomb asymptotic behavior and where the kernel (GV) is not compact. The well-known and successful CCC method, when applied to ($e,3e$) processes, must suffer from analogous problems. Indeed, there the double-continuum wave function is obtained by assuming that the coefficients $C_{n\,\nu}^{L(l\lambda)} = A_n^l B_\nu^\lambda$ in Eq. (19), where the coefficients A_n result from the diagonalization of the matrix of the two-body Hamiltonian describing the subsystem $e + \text{He}^{++}$. Such operation replaces the two-body continuum by a discrete number of pseudostates with positive energies. As Berakdar underlines in [14], the four-body Green's function expansion approach should also face the problem of the noncompactness of the kernel of the LS equation used.

IV. CONCLUSIONS AND PERSPECTIVES

In this paper, we have applied the Jacobi matrix method to the Faddeev-Merkuriev differential equations in order to calculate the three-body wave function that describes the double continuum of an atomic two-electron system. In order to test this wave function, we performed a first-order Born calculation of the fully differential cross section for electron-impact double ionization of helium. In particular, we considered in detail the coplanar kinematics that have been treated experimentally by the group of Lahmam-Bennani. These kinematics involve a very high incident energy, a very small momentum transfer, and very low ejected electron energies.

Our double-continuum wave function which is the solution of a Lippmann-Schwinger equation contains two terms: a free term that satisfies the correct asymptotic conditions in the two-body scattering regions and a correction term involving Green's function and a potential which is in principle of short range. Quite unexpectedly, the results obtained by neglecting the correction term are already in satisfactory agreement with all the experimental data. This agreement is further improved when the correction term is included. We want to stress that in all cases and in particular when the electrons are emitted with the lowest energy, our results do not need to be scaled to be compared to the experimental data, in contrast to all the other methods.

We have also examined the convergence of our results with respect to the basis size. The convergence is reached in terms of the number of electron angular momenta. In terms of the total number of Sturmian functions, the results seem to converge for small values of this number, but the convergence deteriorates for larger values. This problem is related to the noncompactness of the kernel of the Lippmann-Schwinger equation and to the fact that the free term does not satisfy the correct asymptotic conditions in the true three-body scattering region. It is important to note that any approach where the free term does not obey the correct three-body Coulomb asymptotics and where the kernel of the Lippmann-Schwinger equation is not compact cannot pretend to be a mathematically blameless description of the three-body continuum.

One way to overcome the problem of the compactness of the kernel could be the use of the BBK wave function as the free term in the Lippmann-Schwinger equation and to work in parabolic coordinates. In this way, it is known that the potential that enters the correction term has a short range. We are presently working on this approach. On the other hand, it is instructive to mention that the problem of removing the divergences from the Lippmann-Schwinger equation by cutting the long-range potential is discussed up to now even in the two-body case. In this context, a calculation based on the ECS method is desirable. We also plan to replace the free term by a product of two Coulomb functions with, in the case of helium, an effective charge equal to 2 and cut at large distances the dielectronic interaction potential that enters the kernel of the Lippmann-Schwinger equation. This approach will be applied to the treatment of $(e,3e)$ processes with unequal electron energy sharing and to the double ionization of helium by photon impact. Finally, let us stress that methods that do not rely on the Lippmann-Schwinger equation such as the time-dependent approach initiated by Serov [10] should be developed further. In this approach, the total wave packet of the system can reach the genuine asymptotic zone where the different ionization channels are decoupled, allowing a much easier extraction of the relevant information about the ionization processes.

[1] G. Tanner, K. Richter, and J.-M. Rost, Rev. Mod. Phys. **72**, 497 (2000).

[2] J. Eiglsperger, B. Piraux, and J. Madroñero, Phys. Rev. A **80**, 022511 (2009).

[3] H. Bräuning *et al.*, J. Phys. B **31**, 5149 (1998).

[4] A. Kheifets, I. Bray, A. Lahmam-Bennani, A. Duguet, and I. Taouil, J. Phys. B **32**, 5047 (1999).

[5] A. S. Kheifets and I. Bray, Phys. Rev. A **69**, 050701(R) (2004).

[6] L. Malegat, P. Selles, and A. K. Kazansky, Phys. Rev. Lett. **85**, 4450 (2000).

[7] P. Selles, L. Malegat, and A. K. Kazansky, Phys. Rev. A **65**, 032711 (2002).

[8] C. W. McCurdy, M. Baertschy, and T. N. Rescigno, J. Phys. B **37**, R137 (2004); C. W. McCurdy, D. A. Horner, T. N. Rescigno, and F. Martin, Phys. Rev. A **69**, 032707 (2004).

[9] D. Proulx and R. Shakeshaft, Phys. Rev. A **48**, R875 (1993).

[10] V. V. Serov, V. L. Derbov, B. B. Joulakian, and S. I. Vinitsky, Phys. Rev. A **75**, 012715 (2007).

[11] J. Colgan, M. S. Pindzola, and F. Robicheaux, J. Phys. B **34**, L457 (2001).

[12] E. Foumouo, G. L. Kamta, G. Edah, and B. Piraux, Phys. Rev. A **74**, 063409 (2006).

[13] A. Lahham-Bennani, I. Taouil, A. Duguet, M. Lecas, L. Avaldi, and J. Berakdar, Phys. Rev. A **59**, 3548 (1999).

[14] J. Berakdar, Phys. Rev. Lett. **85**, 4036 (2000).

[15] S. Jones and D. H. Madison, Phys. Rev. Lett. **91**, 073201 (2003).

[16] S. A. Zaytsev, V. A. Knyr, and Yu. V. Popov, Phys. At. Nucl. **70**, 676 (2007).

[17] O. Chuluunbaatar, I. V. Puzynin, P. S. Vinitsky, Yu. V. Popov, K. A. Kouzakov, and C. Dal Cappello, Phys. Rev. A **74**, 014703 (2006).

[18] Z. Papp and W. Plessas, Phys. Rev. C **54**, 50 (1996).

[19] Z. Papp, J. Darai, C. Y. Hu, Z. T. Hlousek, B. Kónya, and S. L. Yakovlev, Phys. Rev. A **65**, 032725 (2002).

[20] Z. Papp, J. Darai, J. Z. Mezei, Z. T. Hlousek, and C. Y. Hu, Phys. Rev. Lett. **94**, 143201 (2005).

[21] J. Z. Mezei and Z. Papp, Phys. Rev. A **73**, 030701(R) (2006).

[22] Z. Papp and C. Y. Hu, Phys. Rev. A **66**, 052714 (2002).

[23] S. A. Zaytsev, V. A. Knyr, Yu. V. Popov, and A. Lahmam-Bennani, Phys. Rev. A **75**, 022718 (2007).

[24] S. P. Merkuriev and L. D. Faddeev, *Quantum Scattering Theory for Several Particle Systems* (Kluwer Academic, Dordrecht, 1993).

[25] R. K. Peterkop, *Theory of Ionization of Atoms by Electron Impact* (Colorado Associated University, Boulder, 1977).

[26] R. Gersbacher and J. T. Broad, J. Phys. B **23**, 365 (1990).

[27] E. J. Heller and H. A. Yamani, Phys. Rev. A **9**, 1201 (1974); H. A. Yamani and L. Fishman, J. Math. Phys. **16**, 410 (1975); J. T. Broad and W. P. Reinhardt, Phys. Rev. A **14**, 2159 (1976).

[28] E. J. Heller, Phys. Rev. A **12**, 1222 (1975).

[29] J. T. Broad, Phys. Rev. A **31**, 1494 (1985).

[30] R. Shakeshaft, Phys. Rev. A **70**, 042704 (2004).

[31] G. W. F. Drake, *Handbook of Atomic, Molecular and Optical Physics* (Springer, New York, 2006).

[32] V. A. Knyr, S. A. Zaytsev, Yu. V. Popov, and A. Lahmam-Bennani, in *The J-matrix Method: Recent Developments and Selected Applications*, edited by A. Alhaidari, E. J. Heller, H. A. Yamani, and M. S. Abdelmonem (Springer, Dordrecht, 2008), p. 137.

[33] M. Brauner, J. S. Briggs, and H. Klar, J. Phys. B **22**, 2265 (1989).

[34] L. U. Ancarani, C. Dal Cappello, and G. Gasaneo, J. Phys. Conf. Ser. **212**, 012025 (2010).

[35] C. Dupré, A. Lahmam-Bennani, A. Duguet, F. Mota-Furtado, P. F. O'Mahony, and C. Dal Cappello, J. Phys. B **25**, 259 (1992).

[36] E. J. Weiniger, Comput. Phys. Rep. **10**, 191 (1989).

[37] Z. Papp, Phys. Rev. C **38**, 2457 (1988).

[38] B. A. Lippmann, Phys. Rev. **102**, 264 (1956).

[39] S. Weinberg, Phys. Rev. **133**, B232 (1964).

[40] L. D. Faddeev, *Mathematical Aspects of the Three-Body Problem* (Davey, New York, 1965).

[41] A. M. Mukhamedzhanov, E. O. Alt, and G. V. Avakov, Phys. Rev. C **61**, 064006 (2000).

[42] A. M. Mukhamedzhanov, E. O. Alt, and G. V. Avakov, Phys. Rev. C **63**, 044005 (2001).

[43] A. S. Kadyrov, I. Bray, A. M. Mukhamedzhanov, and A. T. Stelbovics, Ann. Phys. (NY) **324**, 1516 (2009).

[44] S. L. Yakovlev and Z. Papp, Theor. Math. Phys. **163**, 666 (2010).